Dissociation of Acetone Radical Cation ($CH_3COCH_3^{+\cdot} \rightarrow CH_3CO^+ + CH_3^{\cdot}$): An Ab Initio Direct Classical Trajectory Study of the Energy Dependence of the Branching Ratio†

Jia Zhou and H. Bernhard Schlegel*

Department of Chemistry, Wayne State University, Detroit, Michigan 48202

Received: June 30, 2008; Revised Manuscript Received: September 5, 2008

The nonstatistical dissociation of acetone radical cation has been studied by ab initio direct classical trajectory calculations at the MP2/6-31G(d) level of theory. A bond additivity correction has been used to improve the MP2 potential energy surface (BAC-MP2). The energy dependence of the branching ratio, dissociation kinetics, and translational energy distribution for the two types of methyl groups have been investigated using microcanonical ensembles and specific mode excitation. In each case, the dissociation favors the loss of the newly formed methyl group, in agreement with the experiments. For microcanonical ensembles, the branching ratios for methyl loss are calculated to be 1.43, 1.88, 1.70, and 1.50 for 1, 2, 10, and 18 kcal/mol of excess energy, respectively. The energy dependence of the branching ratio is seen more dramatically in the excitation of individual modes involving C−C−O bending. For modes 3 and 6, the branching ratio rises to 1.6 and 1.8−2.3 when 1 or 2 kcal/mol are added, respectively, but falls off when more energy is added. For mode 8, the branching ratio continues to rise monotonically from 1.5 to 2.76 when 1−8 kcal/mol of excess energy are added.

Introduction

The nonstatistical dissociation of acetone radical cation has been the subject of a number of experimental and theoretical studies over the past 35 years. Isomerization from the more stable enol form to the keto isomer leads to chemical activation of the newly formed methyl group which dissociates preferentially. The gas phase chemistry and nonergodic behavior of $C_3H_6O^{\bullet+}$ ions has been reviewed by McAdoo.[1] The enol form of acetone radical cation can be generated from higher aliphatic ketones via the McLafferty rearrangement or by cycloreversion of 1-methlcyclobutanol (Scheme 1).[2]

The enol form of the acetone cation can isomerize to the keto form and then dissociate to produce acetyl cation and methyl radical (Scheme 2). The dissociation reaction proceeds nonergodically, favoring the departure of the newly formed methyl group.

The average ratio for the loss of the active methyl versus loss of the spectator methyl was observed to be ca. 1.4:1,[3−6] whereas RRKM theory would predict that the two methyl groups should dissociate at equal rates.[2,3,7−10] This indicates that randomization of the internal energy is incomplete before dissociation occurs.

Preferential loss of the active methyl group has been seen in collisional activation, electron impact and metastable ion experiments.[1] The energy dependence of the nonstatistical dissociation was studied by Osterheld and Brauman by infrared multiphoton dissociation of acetone enol cation.[6] A branching ratio of 1.16 was found at ca. 0−3 kcal mol^{-1} above threshold and increased to 1.55 at an estimated energy of 8−12 kcal/mol above the barrier. They attribute the increase in branching ratio to the excitation of a mode other than the reaction coordinate, possibly the C−C−O bending involving the spectator methyl group.

Recent photoionizantion[11] and TPEPICO[12] experiments yield 18.5 ± 0.5 kcal/mol for the energy difference between

SCHEME 1

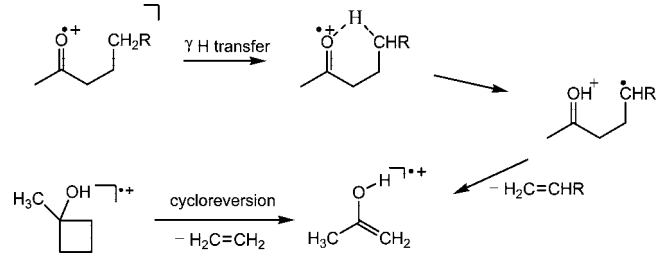

SCHEME 2

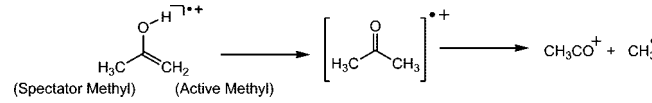

$CH_3COCH_3^{\bullet+}$ and $CH_3CO^+ + CH_3^{\bullet}$ at 0 K. This is slightly lower than the previous experimental value 19.8 ± 0.3 kcal/mol.[13] A number of groups have used ab initio calculations to explore the potential energy surface for $CH_3COCH_3^{\bullet+}$.[11,14,15] The experimental values for $CH_3COCH_3^{\bullet+} \rightarrow CH_3CO^+ + CH_3^{\bullet}$ fall between the best calculated values, 17.7, 17.9, 21.1 and 20.6 kcal/mol for G2MP2,[14] G3,[11] CBS-QB3[15] and CBS-APNO,[15] respectively. The best estimates for the keto to enol isomerization barrier $CH_3COCH_3^{\bullet+}$ at 0 K are 36.0, 36.6, 35.8 and 34.7 kcal/mol for G2MP2,[14] G3,[11] CBS-QB3[15] and CBS-APNO,[15] respectively.

The nonstatistical dynamics of acetone radical cation dissociation has been studied by quasiclassical trajectory calculations. Nummela and Carpenter[16] used semiempirical AM1 calculations with specific reaction parameters (AM1-SRP) and obtained a branching ratio of 1.13 ± 0.09 for dissociation of the active versus the spectator methyl group. The trajectories were started at the transition state for keto−enol tautomeriztion and were sampled from a microcanonical distribution with 10 kcal/mol energy in excess of the zero

† Part of the "Sason S. Shaik Festschrift".

10.1021/jp8057492 CCC: $40.75
Published on Web 10/24/2008

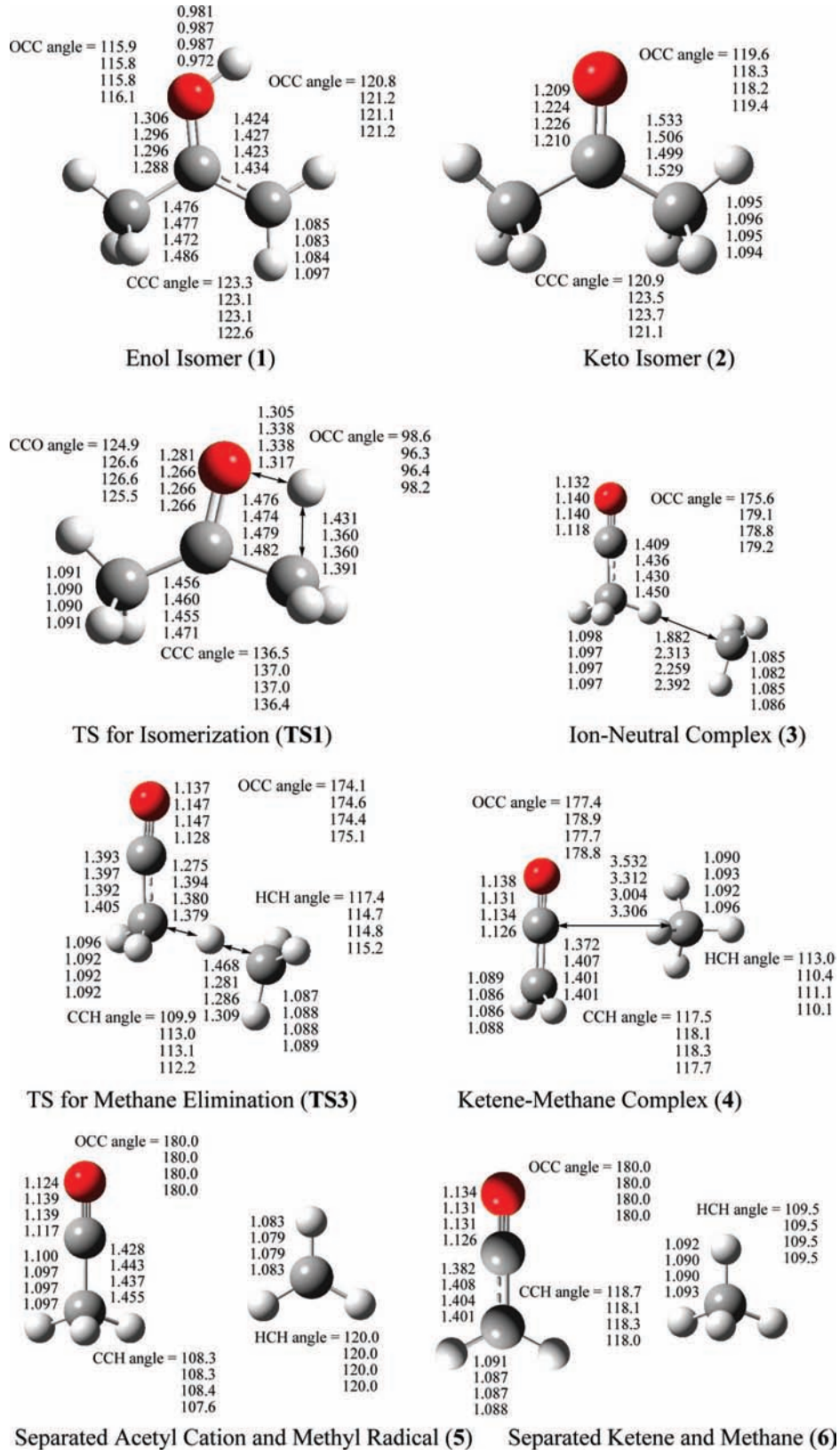

Figure 1. Structures and selected geometric parameters of stationary points on the acetone radical cation potential energy surface optimized at the TPSSTPSS/cc-pVTZ, MP2/6-31G(d), BAC-MP2/6-31G(d), and QCISD/6-311G(d,p) levels of theory (top row to bottom, respectively). Bond distances are in Å, and angles are in degrees.

point energy of the transition state. Anand and Schlegel[15] found a branching ratio of 1.53 ± 0.20 at the MP2/6-31G(d) level of theory using the same starting conditions. In the present work, we used quasiclassical trajectory calculations at the MP2/6-31G(d) level of theory with bond additivity corrections[17−21] to study the energy dependence of the branching ratio.

TABLE 1: Energies of the Various Points on the Acetone Radical Cation PES[a]

	1	TS1	2	3	TS3	4	5	6	MAD[b]
B3LYP/6-31G(d)	−4.5	37.8	0.0	19.3	19.3	18.3	26.4	22.3	3.2
B3LYP/cc-pVTZ[c]	−10.2	38.1	0.0				24.4		
PBE1PBE/cc-pVTZ	−8.6	33.5	0.0	19.5	19.3	19.9	25.7	24.1	3.1
TPSSTPSS/cc-pVTZ	−5.1	33.3	0.0	15.5	14.9	14.3	23.2	20.3	1.8
MP2/6-31G(d)	−12.2	36.0	0.0	4.6	12.5	9.0	8.5	11.1	5.7
MP2/6-311+G(d,p)	−13.9	34.0	0.0	2.3	8.5	6.4	5.7	9.0	7.7
BAC-MP2/6-31G(d)	−12.6	35.7	0.0	10.4	13.5	13.0	16.2	21.6	2.9
MP3/6-31G(d,p)[d]	−12.0	39.4	0.0	16.1	24.0	16.8	21.0	20.6	2.6
QCISD/6-311G(d,p)[e]	−6.1	40.1	0.0	13.1	20.2	14.5	16.1	16.7	2.1
QCISD(T)/6-311++G(2df,p)[f]	−7.6	36.6	0.0	14.0	18.4	15.0	17.3	17.9	0.8
CBS-QB3	−7.8	35.8	0.0	16.1	18.9	15.4	19.4	18.5	0.3
CBS-APNO	−8.0	35.2	0.0	15.3	18.1	15.1	19.3	18.5	

[a] In kcal/mol at 0 K, relative to **2** (keto isomer). [b] Mean absolute deviation from the CBS-APNO level of theory. [c] Reference 16. [d] Referece 10. [e] With MP2/6-31G(d) zero point energies. [f] QCISD/6-311G(d,p) geometry with MP2/6-31G(d) zero point energies.

TABLE 2: Number of Trajectories for the Dissociation of Acetone Radical Cation

ensemble energy (kcal/mol)	nonreactive (enol/keto)	active methyl	spectator methyl	ratio (active:spectator)
1	63/52	109	76	1.43:1
2	36/34	150	80	1.88:1
10	11/39	126	74	1.70:1
18	9/28	120	80	1.50:1

Method

The Gaussian[22] suite of programs was employed to carry out the ab initio electronic structure and molecular dynamics calculations. The geometries of the minima and the transition states have been optimized previously[15] by Hartree−Fock theory (HF), density functional theory (DFT), second-order Møller−Plesset perturbation theory (MP2) and quadratic configuration interaction with single and double excitations (QCISD).[23] The density functionals use in this work include two hybrid GGA (generalized gradient approximation) functionals, B3LYP[24,25] and PBE1PBE,[26] and a meta-GGA, TPSSTPSS.[27] The complete basis set extrapolation methods (CBS-QB3 and CBS-APNO) of Petersson and co-workers[28] were used to compute accurate energy differences. The CBS-APNO calculations have a mean absolute deviation of 0.5 kcal/mol for heats of reaction.

Accurate methods such as CBS-APNO are not practical for molecular dynamics corrections, but more affordable methods such as DFT and MP2 may not yield sufficiently accurate energetics. However, the errors are often systematic, e.g., arising from the making and breaking of bonds. The empirical corrections that have been used to correct computed thermochemistry[17−21] can also be employed to improve potential energy surfaces for molecular dynamics calculations.[29] As in the BAC-MP4 method,[21] a simple exponential is used to correct the potential for bond dissociations. In the present case, the bond additivity correction (BAC) is applied only to the C−C bonds for the dissociation of the active and spectator methyl groups:

$$\Delta E_{\mathrm{BAC}} = A \exp(-\alpha R_{\mathrm{CC1}}) + A \exp(-\alpha R_{\mathrm{CC2}}) \qquad (1)$$

The parameters $A = -0.028$ and $\alpha = 0.196$ are obtained by fitting the MP2/6-31G(d) energetics to the CBS-APNO level of theory. The structures used in the fit include the transition state (TS) for enol−keto isomerization, the keto isomer, and the methyl dissociation products. The corresponding first and second derivatives of ΔE_{BAC} are added to MP2 gradient and Hessian. This BAC approach has been used previously to study the branching ratios in $CH_2O^{\bullet-} + CH_3Cl \rightarrow CH_3CH_2O^{\bullet} + Cl^-$, $CH_2O + CH_3^{\bullet} + Cl^-$.[29]

Ab initio classical trajectories were computed at the BAC-MP2/6-31G(d) level of theory using a Hessian-based predictor-corrector method.[30,31] A predictor step is taken on the quadratic surface obtained from the energy, gradient and Hessian from the beginning point. A fifth-order polynomial is then fitted to the energies, gradients and Hessians at the beginning and end points of the predictor step, and the Bulirsch Stoer algorithm[32] is used to take a corrector step on this fitted surface with the angular forces projected out. The Hessians are updated for 5 steps before being recalculated analytically.[30] The trajectories were terminated when the centers of mass of the fragments were 8 bohr apart and the gradient between the fragments was less than 1×10^{-5} hartree/bohr. A step size of 0.25 amu$^{1/2}$ bohr was used for integrating the trajectories. The energy was conserved to better than 1×10^{-5} hartree and the angular momentum was conserved to 1×10^{-8} $\hbar$.

Trajectories were initiated at the transition state for the keto−enol tautomerization. For the first part of the study, a microcannonical ensemble of initial states was constructed using quasi-classical normal mode sampling.[33,34] A total energy of 1, 2, 10, and 18 kcal/mol above the zero point energy of the transition state was distributed among the 23 vibrational modes and translation along the transition vector. The total angular momentum was set to zero corresponding to a rotationally cold distribution and the phases of the vibrational modes were chosen randomly. For each initial condition, the momentum and displacement were scaled so that the desired total energy was the sum of the vibrational kinetic energy and the potential energy obtained from the ab initio surface. The initial conditions are similar to those chosen by Nummela and Carpenter.[16] For each case, a total of 200−300 trajectories were integrated for up to 400 *fs* starting at the transition state and ending when the products were well separated. In the second part of the study, 1, 2, 4 and 8 kcal/mol was added to each of 3 selected vibrational modes and 0.5 kcal/mol of translational energy was added to the transition vector, and the remaining modes were given only zero point energy. The remaining conditions were the same as in the first part of the study, and 110 trajectories were integrated for each case. A total of ca. 2500 trajectories were calculated for the 17 different ensembles (200−300 trajectories for each of 4 microcanonical ensembles and 110 trajectories for each of the 13 ensembles for specific mode excitation).

Results and Discussion

Structures and Energetics. Figure 1 shows the optimized geometries of the key structures on the potential energy surface for acetone radical cation dissociation at the TPSS, MP2, BAC-MP2 and QCISD levels of theory. The largest differences are

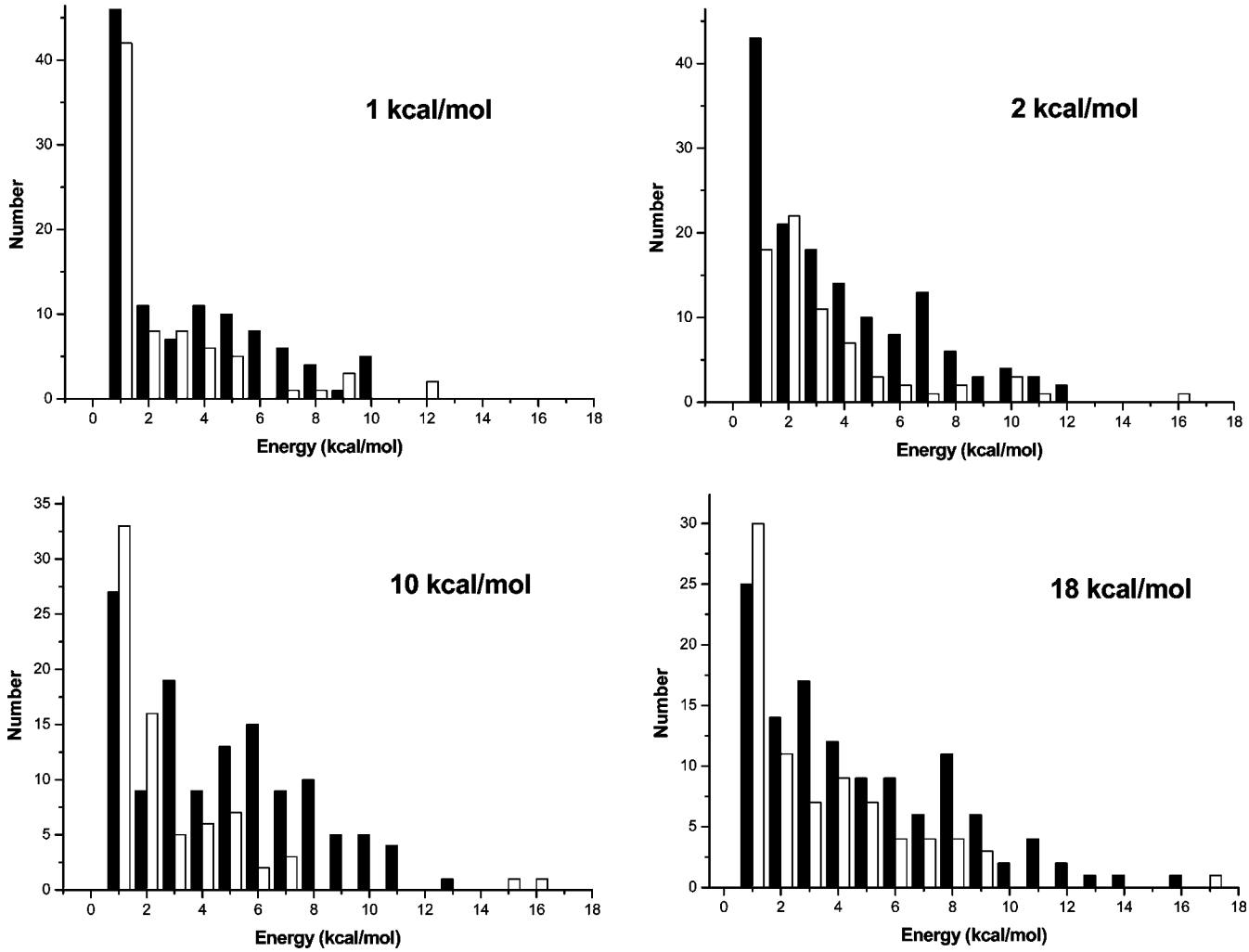

Figure 2. Translational energy distributions of the methyl fragments derived from the active (filled) and spectator (empty) methyl fragments with 1, 2, 10, and 18 kcal/mol excess energies.

TABLE 3: Average Translational Energies *E* (in kcal/mol) and Dissociation Time *T* (in fs)

	active methyl		spectator methyl	
ensemble energy (kcal/mol)	E	T	E	T
1	2.737	181.09	1.996	224.39
2	3.306	177.14	2.705	240.22
10	4.177	147.47	2.256	185.69
18	4.204	139.91	2.833	167.40

the monomer separations in the ion-neutral complexes, **3** and **4**. The transition states calculated by TPSS are somewhat earlier than those calculated by MP2 or QCISD. The bond additivity corrections produce only minor changes in the MP2 geometry. The bond lengths between heavy atoms at TPSS, MP2 and BAC-MP2 have similar mean absolute deviations (ca. 0.01 Å) when compared to the QCISD structures.

The relative energies are collected in Table 1. As can be judged from the mean absolute deviations, the QCISD(T) and CBS-QB3 calculations are in very good agreement with the CBS-APNO calculations. However, ab initio trajectory calculations are not feasible with CBS, QCI or MP3 methods. The methyl dissociation energy is too low at the MP2 level but is much improved at the BAC-MP2 level. The TPSS calculations with a large basis set perform significantly better than B3LYP or PBE. However, trajectory calculations with the TPSS/cc-pVTZ level of theory are estimated to be ca. 10 times more expensive than the BAC-MP2 trajectories. The B3LYP/6-31G(d) is comparable in cost to BAC-MP2/6-31G(d). However, B3LYP/6-31G(d) places the $CH_2CO^+ + CH_4$ channel (**6**) substantially below the $CH_3CO^+ + CH_3$ channel (**5**). This cannot be fixed with a simple bond additivity correction involving only the two C−C bonds. Although higher levels of theory would provide a more accurate description of the potential energy surface, the BAC-MP2 level is a reasonable compromise between accuracy and affordability that allows us calculate the ca. 2500 trajectories needed to explore the energy dependence of the branching ratio.

Dynamics. ***Microcanonical Ensemble.*** Four sets of initial conditions were constructed with 1, 2, 10, and 18 kcal/mol above the zero point energy of the transition state. The results of the trajectory calculations for the dissociation of acetone radical cation are listed in Table 2. For the 300 trajectories of with 1 kcal/mol extra energy, 109 resulted in the loss of the active methyl and 76 finished with the loss of the spectator methyl. The remaining 115 trajectories either went to the enol isomer (63 trajectories) or stayed near the keto minimum (52 trajectories), not meeting the stopping criteria within 400 fs. Of the 300 trajectories integrated with 2 kcal/mol extra energy, 150 resulted in the loss of the active methyl and 80 finished with the loss of the spectator methyl. Integration of 250 trajectories of with 10 kcal/mol extra energy yielded 126 active methyl dissociations and 74 spectator methyl dissociations. The 237 trajectories with 18 kcal/mol extra energy resulted in 120 active

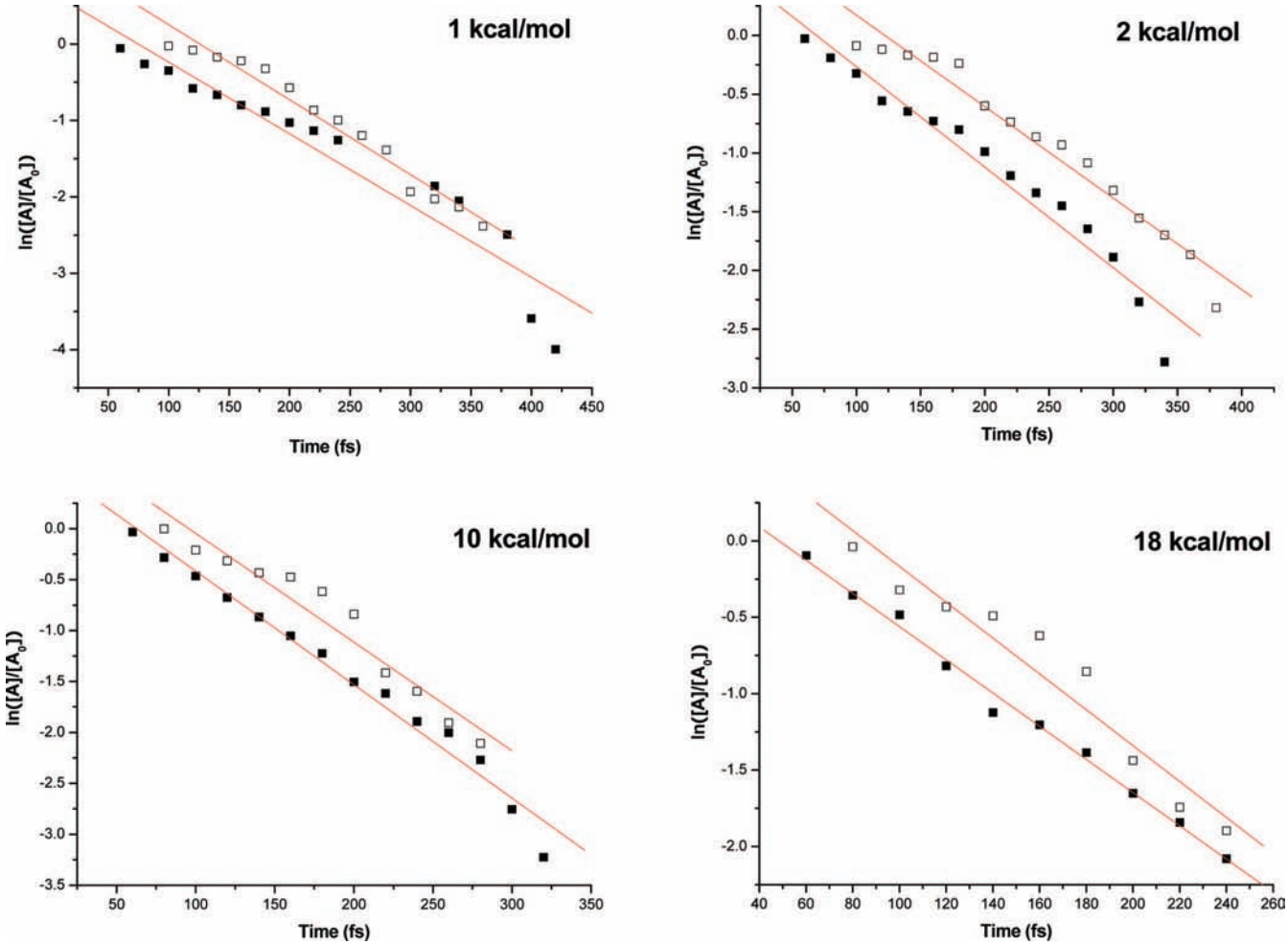

Figure 3. Plot showing the first-order kinetics for active (filled) and spectator (empty) methyl fragments dissociation with 1, 2, 10, and 18 kcal/mol excess energies.

methyl loses and 80 spectator methyl loses. As the energy of the microcanonical ensemble is increased from 1 to 2 kcal/mol, the branching ratio for active to spectator methyl group increases from 1.43 to 1.88. However, when the energy of the microcanonical ensemble continues to increase from 2 to 10 to 18 kcal/mol, the branching ratio for active to spectator methyl group decreases from 1.88 to 1.70 to 1.50. In contrast, in the experiments of Osterheld and Brauman[6] the branching ratio increases with increasing laser intensity and then seems to reach a plateau. This suggests that energy may be deposited preferentially in specific modes, rather than uniformly in all of the vibrational modes. This will be examined in the second part of the study (see below).

At each energy in the microcanonical simulations on the BAC-MP2 surface, a number of trajectories stayed in the keto minimum, whereas in the previous study at the MP2 level without bond additivity corrections, none of the trajectories remained in the keto minimum. The MP2/6-31G(d) level of theory underestimates C−C bond energy of keto isomer in comparison to CBS-APNO, permitting the methyl group to dissociate more easily. The BAC-MP2/6-31G(d) calculations yield a higher methyl dissociation energy, and some trajectories cannot overcome the barrier for dissociation to the products within the simulation time. The higher barrier at the BAC-MP2/6-31G(d) level is much closer to experiment and the CBS-APNO calculations, and hence the dynamics should be more realistic at this level of theory.

The calculated translational energy distributions are plotted in Figure 2. The majority of methyl groups have a translational energy less than 4 kcal/mol. Of the methyl groups with larger translational energies, many come from dissociation of the active methyl. As indicated in Table 3, the active methyl has a larger average translational energy than spectator methyl. Experimentally, the kinetic energy releases for the active and spectator methyl groups are 5.0 and 4.3 kcal/mol, respectively.[8] As the total extra energy increases, the average translational energy of the active methyl group increases more than that of the spectator methyl group. Table 3 also lists the average dissociation times. The dissociation time is taken as the time when the C−C bond reaches 3.0 Å, provided that the methyl group does not return to form the C−C bond again. The average dissociation times generally decrease with increasing energy, and the average time for the active methyl dissociation time is always shorter than for the spectator methyl. Just as the branching ratio increases first and then decreases with increasing energy, the ratio of the spectator to active methyl group average dissociation times also has the same trend with increasing energy.

Figure 3 plots the logarithm of the number of undissociated acetone radical cations versus time. The nearly linear plots are indicative of first-order kinetics as expected for unimolecular dissociation. The spectator methyl groups generally needed more time to dissociate than the active methyl, validating the result of average dissociation time listed in Table 3.

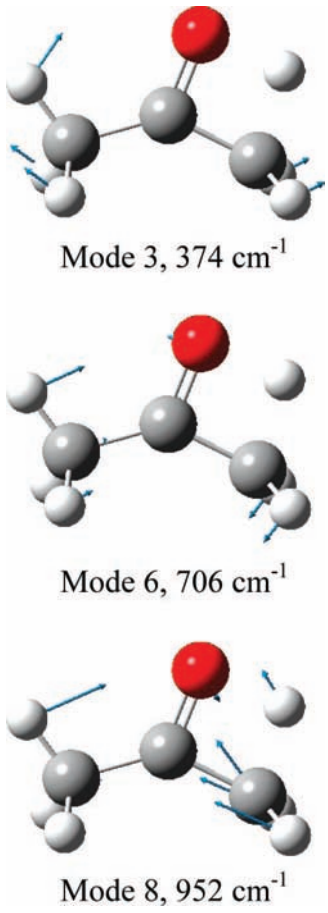

Figure 4. Displacement vectors for vibrational modes 3, 6, and 8, along with corresponding vibrational frequencies.

TABLE 4: Branching Ratio for Exciting Specific Modes[a]

ensemble energy (kcal/mol)	mode 3	mode 6	mode 8
0	1.10:1	1.10:1	1.10:1
1	1.59:1	1.58:1	1.54:1
2	1.84:1	2.31:1	1.82:1
4	1.46:1	1.85:1	2.36:1
8	1.55:1	2.03:1	2.76:1

[a] Zero point energy in the remaining vibrational modes and 0.5 kcal/mol in the transition vector.

Excitation of Specific Modes. Osterheld and Brauman suggested that the increase in branching ratio with laser intensity was due to the excitation of specific vibrational modes. In particular, they indicated that the C−C−O bending modes may be suitable candidates. An examination of the vibrations of the TS for enol−keto isomerization yields three modes involving C−C−O bending, as shown in Figure 4. For each mode, four ensembles were constructed with 1, 2, 4, and 8 kcal/mol of excess energy in the specific mode, 0.5 kcal/mol in the transition vector, and zero point energy in all modes. For comparison, one ensemble was also constructed without specific mode excitation, having only 0.5 kcal/mol in the transition vector and zero point energy in each of the vibrational modes. For each set, a total of 110 trajectories were integrated.

The branching ratio for the various cases of specific mode excitation can be found in Table 4. If only 0.5 kcal/mol is added in the transition vector, the branching ratio is 1.10:1. This indicates that the energy released in descending from the transition state to the keto minimum is not deposited efficiently in the modes favoring the dissociation of the active methyl group. For each of the three modes involving C−C−O bending, the branching ratio increases to 1.5:1 when as little as 1 kcal/mol extra energy is in the mode. Adding 2 kcal/mol to any of the three modes increases the branching ratio to 1.8−2.3. Depositing energy in mode 8 is the most effective of the three modes examined. Adding more energy to mode 3 and 6 actually decreases the branching ratio. This parallels the study using a microcanonical ensemble, in which the branching ratio decreases when more than 2 kcal/mol extra energy is added. Most likely, specific excitation of other vibrational mode will alter the branching ratio as well.

Conclusions

The energy dependence of the branching ratio for acetone radical cation has been investigated by ab initio direct classical trajectory calculations. The MP2/6-31G(d) level of theory with bond additivity corrections gives a better potential energy surface than the MP2 and B3LYP levels of theory when compared to the CBS-APNO results. The nonstatistical dissociation of acetone radical cation has been studied using microcanonical ensembles and specific mode excitation. For microcanonical ensembles, the ratios of methyl radical production from the newly formed (active) methyl to the existing (spectator) methyl are 1.43, 1.88, 1.70, and 1.50 for 1, 2, 10, and 18 kcal/mol of excess energy, respectively. The dissociations generally obey first-order unimolecular kinetics. The active methyl usually carries more kinetic energy than spectator methyl, and the average dissociation time of active methyl is less than that of spectator methyl. Three vibrations involving C−C−O bending were chosen for the specific mode excitation. In each case, the branching ratio increases when 1 or 2 kcal/mol was added. For two of the modes, the branching ratio decreased when more than 2 kcal/mol energy was added, similar to the study of microcanonical ensembles. However, for mode 8, the branching ratio continued to increase with added energy, reaching a ratio of 2.76:1 with 8 kcal/mol of excess energy.

Acknowledgment. This work was supported by grant from the National Science Foundation (CHE 0512144). Computer time on the Wayne State University grid is gratefully acknowledged.

References and Notes

(1) McAdoo, D. J. *Mass Spectrom. Rev.* **2000**, *19*, 38–61.
(2) McLafferty, F. W.; McAdoo, D. J.; Smith, J. S.; Kornfeld, R. *J. Am. Chem. Soc.* **1971**, *93*, 3720–30.
(3) Depke, G.; Lifshitz, C.; Schwarz, H.; Tzidony, E. *Angew. Chem. Int. Ed* **1981**, *20*, 792–793.
(4) McAdoo, D. J.; Hudson, C. E. *Int. J. Mass Spectrom. Ion Processes* **1984**, *59*, 77–83.
(5) Turecek, F.; Hanus, V. *Org. Mass Spectrom.* **1984**, *19*, 631–638.
(6) Osterheld, T. H.; Brauman, J. I. *J. Am. Chem. Soc.* **1993**, *115*, 10311–16.
(7) Lifshitz, C.; Berger, P.; Tzidony, E. *Chem. Phys. Lett.* **1983**, *95*, 109–113.
(8) Lifshitz, C.; Tzidony, E. *Int. J. Mass Spectrom. Ion Processes* **1981**, *39*, 181–95.
(9) Lifshitz, C.; Tzidony, E.; Terwilliger, D. T.; Hudson, C. E. *Adv. Mass Spectrom.* **1980**, *8A*, 859–66.
(10) Heinrich, N.; Louage, F.; Lifshitz, C.; Schwarz, H. *J. Am. Chem. Soc.* **1988**, *110*, 8183–8192.
(11) Wei, L. X.; Yang, B.; Yang, R.; Huang, C. Q.; Wang, J.; Shan, X. B.; Sheng, L. S.; Zhang, Y. W.; Qi, F.; Lam, C. S.; Li, W. K. *J. Phys. Chem. A* **2005**, *109*, 4231–4241.
(12) Rennie, E. E.; Boulanger, A. M.; Mayer, P. M.; Holland, D. M. P.; Shaw, D. A.; Cooper, L.; Shpinkova, L. G. *J. Phys. Chem. A* **2006**, *110*, 8663–8675.
(13) Fogleman, E. A.; Koizumi, H.; Kercher, J. P.; Sztaray, B.; Baer, T. *J. Phys. Chem. A* **2004**, *108*, 5288–5294.

(14) Mishima, K.; Hayashi, M.; Lin, S. H. *Int. J. Mass Spectrom.* **2004**, *238*, 1–15.

(15) Anand, S.; Schlegel, H. B. *Phys. Chem. Chem. Phys.* **2004**, *6*, 5166–5171.

(16) Nummela, J. A.; Carpenter, B. K. *J. Am. Chem. Soc.* **2002**, *124*, 8512–8513.

(17) Allendorf, M. D.; Melius, C. F. *J. Phys. Chem. A* **2005**, *109*, 4939–4949.

(18) Anantharaman, B.; Melius, C. F. *J. Phys. Chem. A* **2005**, *109*, 1734–1747.

(19) Ho, P.; Coltrin, M. E.; Binkley, J. S.; Melius, C. F. *J. Phys. Chem.* **1985**, *89*, 4647–4654.

(20) Melius, C. F.; Allendorf, M. D. *J. Phys. Chem. A* **2000**, *104*, 2168–2177.

(21) Ho, P.; Melius, C. F. *J. Phys. Chem.* **1990**, *94*, 5120–5127.

(22) Frisch, M. J.; Trucks, G. W.; Schlegel, H. B.; Scuseria, G. E.; Robb, M. A.; Cheeseman, J. R.; Montgomery, J. A., Jr.; Vreven, T.; Scalmani, G.; Mennucci, B.; Barone, V.; Petersson, G. A.; Caricato, M.; Nakatsuji, H.; Hada, M.; Ehara, M.; Toyota, K.; Fukuda, R.; Hasegawa, J.; Ishida, M.; Nakajima, T.; Honda, Y.; Kitao, O.; Nakai, H.; Li, X.; Hratchian, H. P.; Peralta, J. E.; Izmaylov, A. F.; Kudin, K. N.; Heyd, J. J.; Brothers, E.; Staroverov, V.; Zheng, G.; Kobayashi, R.; Normand, J.; Sonnenberg, J. L.; Iyengar, S. S.; Tomasi, J.; Cossi, M.; Rega, N.; Burant, J. C.; Millam, J. M.; Klene, M.; Knox, J. E.; Cross, J. B.; Bakken, V.; Adamo, C.; Jaramillo, J.; Gomperts, R.; Stratmann, R. E.; Yazyev, O.; Austin, A. J.; Cammi, R.; Pomelli, C.; Ochterski, J. W.; Ayala, P. Y.; Morokuma, K.; Voth, G. A.; Salvador, P.; Dannenberg, J. J.; Zakrzewski, V. G.; Dapprich, S.; Daniels, A. D.; Strain, M. C.; Farkas, O.; Malick, D. K.; Rabuck, A. D.; Raghavachari, K.; Foresman, J. B.; Ortiz, J. V.; Cui, Q.; Baboul, A. G.; Clifford, S.; Cioslowski, J.; Stefanov, B. B.; Liu, G.; Liashenko, A.; Piskorz, P.; Komaromi, I.; Martin, R. L.; Fox, D. J.; Keith, T.; Al-Laham, M. A.; Peng, C. Y.; Nanayakkara, A.; Challacombe, M.; Chen, W.; Wong, M. W.; Pople, J. A. *Gaussian*, revision F.02; Gaussian, Inc.: Wallingford, CT, 2007.

(23) Pople, J. A.; Head-Gordon, M.; Raghavachari, K. *J. Chem. Phys.* **1987**, *87*, 5968–5975.

(24) Becke, A. D. *J. Chem. Phys.* **1993**, *98*, 1372–1377.

(25) Lee, C.; Yang, W.; Parr, R. D. *Phys. Rev. B* **1988**, *37*, 785–789.

(26) Perdew, J. P.; Burke, K.; Ernzerhof, M. *Phys. Rev. Lett.* **1996**, *77*, 3865–3868.

(27) Tao, J. M.; Perdew, J. P.; Staroverov, V. N.; Scuseria, G. E. *Phys. Rev. Lett.* **2003**, *91*, 146401.

(28) Montgomery, J. A.; Ochterski, J. W.; Peterson, G. A. *J. Chem. Phys.* **1994**, *101*, 5900–5909.

(29) Li, J.; Shaik, S.; Schlegel, H. B. *J. Phys. Chem. A* **2006**, *110*, 2801–2806.

(30) Bakken, V.; Millam, J. M.; Schlegel, H. B. *J. Chem. Phys.* **1999**, *111*, 8773–8777.

(31) Millam, J. M.; Bakken, V.; Chen, W.; Hase, W. L.; Schlegel, H. B. *J. Chem. Phys.* **1999**, *111*, 3800–3805.

(32) Stoer, J.; Bulirsch, R. *Introduction to Numerical Analysis*; Springer-Verlag: New York, 1980.

(33) Hase, W. L. In *Encyclopedia of Computational Chemistry*; Schleyer, P. v. R., Allinger, N. L., Clark, T., Gasteiger, J., Kollman, P. A., Schaefer, H. F., III, Schreiner, P. R., Eds.; Wiley: Chichester, U.K., 1998; pp 402−407.

(34) Peslherbe, G. H.; Wang, H.; Hase, W. L. *Adv. Chem. Phys.* **1999**, *105*, 171–201.

JP8057492